Electronic Supplementary Material (ESI) for New Journal of Chemistry.

Supplementary Information for

Electrochemically assisted synthesis of poly (3, 4-dihydroxyphenylalanine) fluorescent organic nanoparticles for sensing applications

Haidong Li[a,*], Miaoxia Liu[a], Ruhan Qiu[b], Zongping Liu[b], Chengyin Wang[a,*], Guoxiu Wang[c,*]

[a] School of Chemistry and Chemical Engineering, Yangzhou University, Yangzhou, Jiangsu, 225002, China

[b] College of Veterinary Medicine, Yangzhou University, Yangzhou, Jiangsu, 225009, China

[c] Centre for Clean Energy Technology, University of Technology Sydney, City Campus, Broadway, Sydney, NSW 2007, Australia

Corresponding authors:

Tel: (+86)514-87975590

E-mail addresses: (H. L) haidongligxbb@yzu.edu.cn,

(C. W) wangcy@yzu.edu.cn,

(G. W) guoxiu.wang@uts.edu.au

1 Apparatus

Absorption spectra were measured by a UV-vis 2550 spectrophotometer (Shimadzu, Japan). Fluorescence spectra were recorded by a Hitachi F-7000 Fluorescence Spectrofluorometer (Hitachi, Japan). Fourier transform infrared (FTIR) spectra were performed on a TENSOR 27 spectrophotometer (Bruker, Germany). Transmission electron microscope (TEM) images were acquired by using a JEM-2100 (Japan) with a 200-kV accelerating voltage. X-ray photoelectron spectroscopy (XPS) was carried on an ESCALAB 250Xi X-ray photoelectron spectroscopy (Thermo Scientific, USA). A CHI660B electrochemical workstation (Shanghai CHI Instruments Co., China) was used to conducted cyclic voltammetry (CV) measurements and the electrochemical oxidation by connecting to a three-electrode cell, where a KCl saturated Ag/AgCl electrode as the reference electrode, a platinum wire electrode as the counter electrode and glassy carbon electrode (GCE, 3 mm in diameter) or ITO glass (10 mm × 30 mm) as the working electrode. Prior to use, GCE and ITO were thoroughly clean according to reported procedures.[1, 2]

2. Quantum yield measurement

The fluorescence quantum yield of the polyDOPA-FONs was measured by using quinine sulfate in 0.1 M H_2SO_4 (Φ_R = 0.54 at 360 nm) as a standard reference. Then the equation used to calculate the quantum yield is given as follows:

$$\Phi_x = \Phi_R \times \frac{I_x}{I_R} \times \frac{A_R}{A_x} \times \frac{\eta_x^2}{\eta_R^2}$$

where Φ refers to the fluorescence quantum yield, *I* is the measured integrated emission intensity, A is the ultraviolet absorbance, η is the refractive index of the solvent (1.33 for water), and the subscript x and R represent the sample and the standard reference. The absorbance in a 10-mm cuvette was always kept below 0.1 at the excitation wavelength to minimize the reabsorption effects.

3. Supplementary data

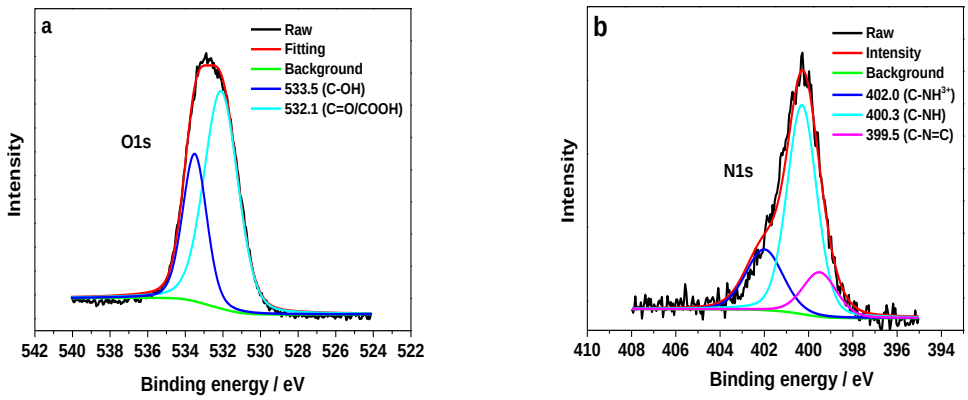

Fig. S1. (a) O 1s spectra of the polyDOPA-FONs. **(b)** N 1s spectra of the polyDOPA-FONs.

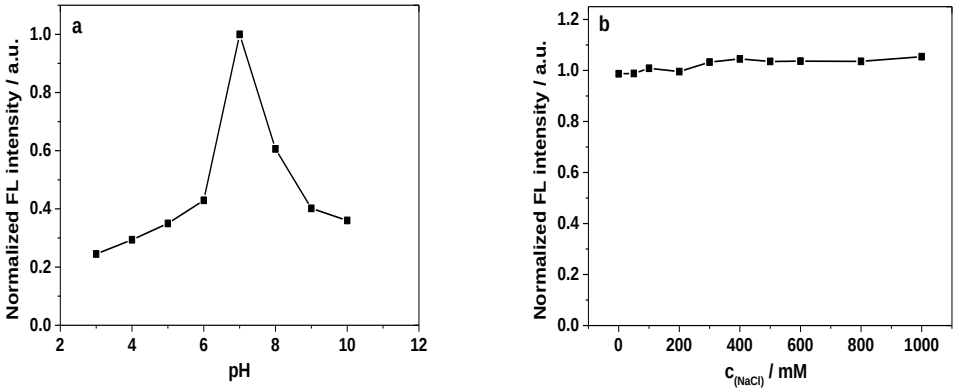

Fig. S2. (a) Effect of pH on the fluorescence intensity. **(b)** Effect of ionic strength on the

fluorescence intensity. The ionic strength of the solution was adjusted by different concentrations of NaCl.

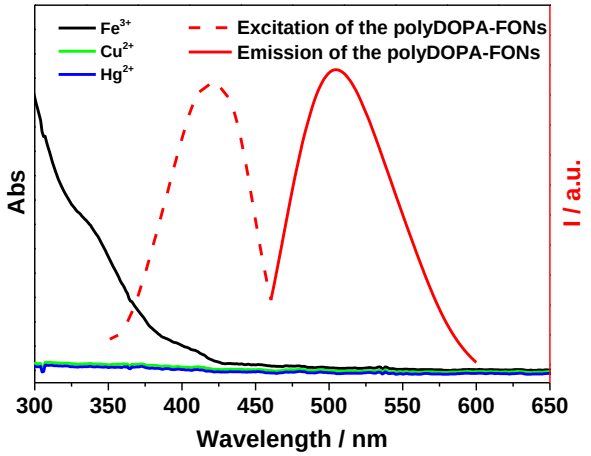

Fig. S3. UV–vis adsorption spectra of $CuCl_2$, $Fe(NO_3)_3$ and $Hg(NO_3)_2$ solutions (100 μM), the fluorescence spectra of the polyDOPA-FONs in water.

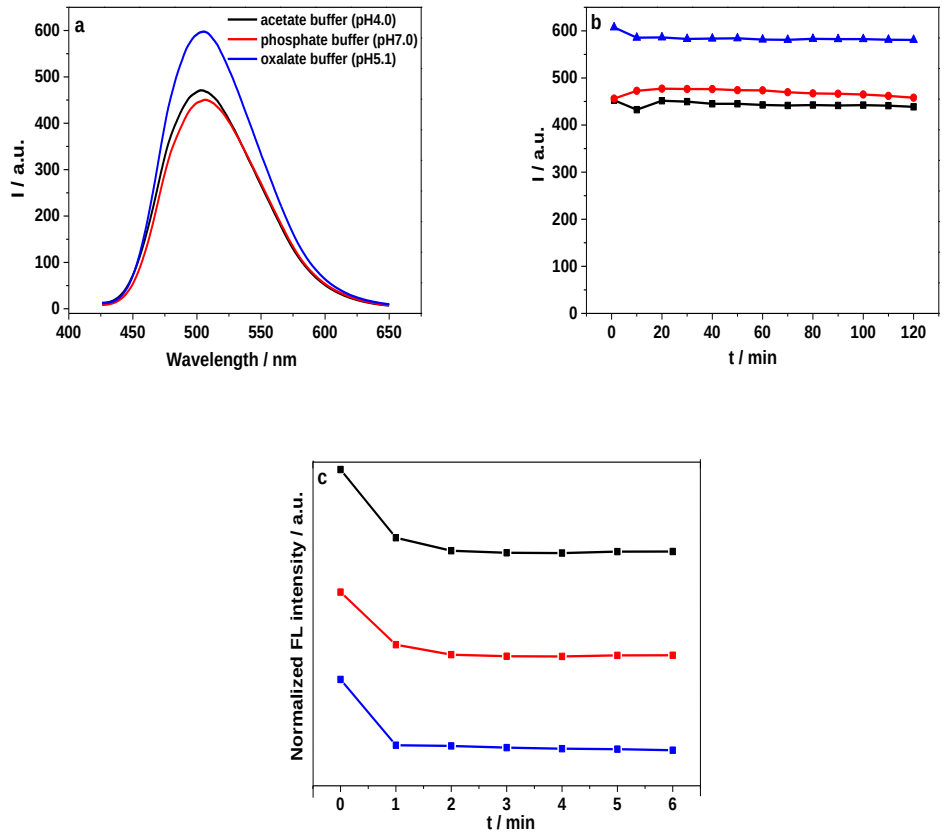

Fig. S4. (a) Fluorescence spectra of the polyDOPA-FONs recorded in three different buffer solutions. **(b)** Photostability of the polyDOPA-FONs in acetate buffer solution (pH 4.0) (back curve), phosphate buffer solution (pH 7.0) (red curve) and oxalate buffer solution (pH 5.1) (blue curve) upon the irradiation by xenon lamps for different time. **(c)** Time-dependent of normalized fluorescence intensity upon the addition of Fe^{3+} (black curve), Cu^{2+} (red curve) and Hg^{2+} (blue curve).

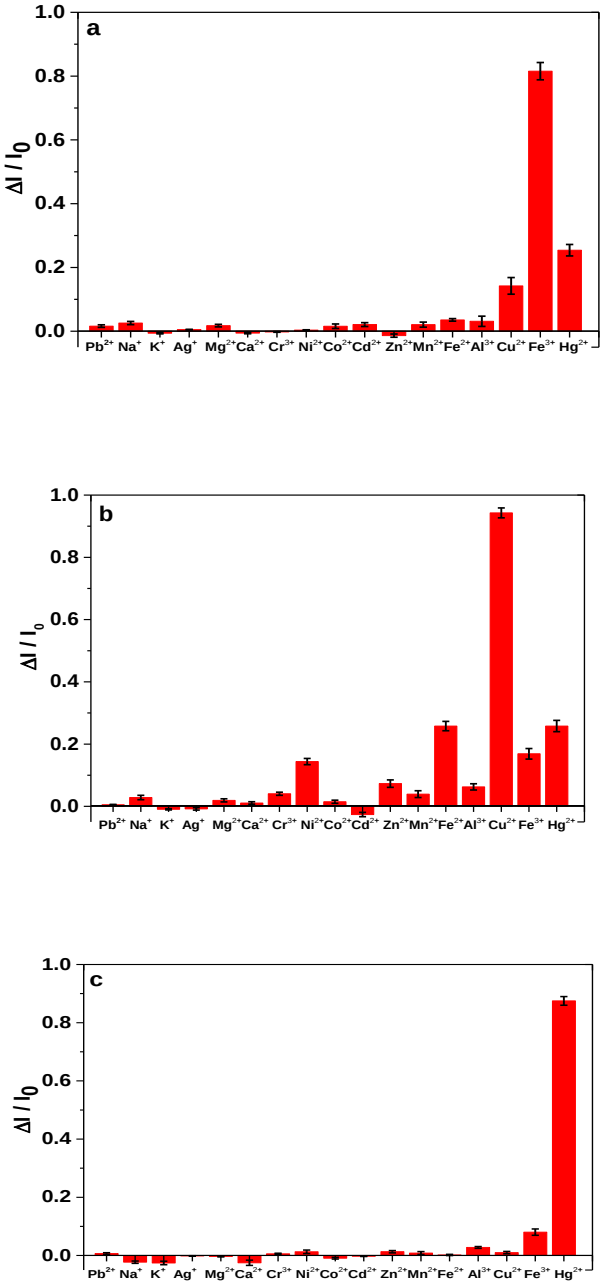

Fig. S5. Comparison of the fluorescence quenching efficiency for different metal ions in (a) acetate buffer solution (0.20 M, pH 4.0), (b) phosphate buffer solution (0.02 M, pH 7.0) and (c) oxalate buffer solution (0.03 M, pH 5.1). The concentration for Fe^{3+}, Cu^{2+} and Hg^{2+} is 10 μM, while the concentration for the other metal ions is 100 μM.

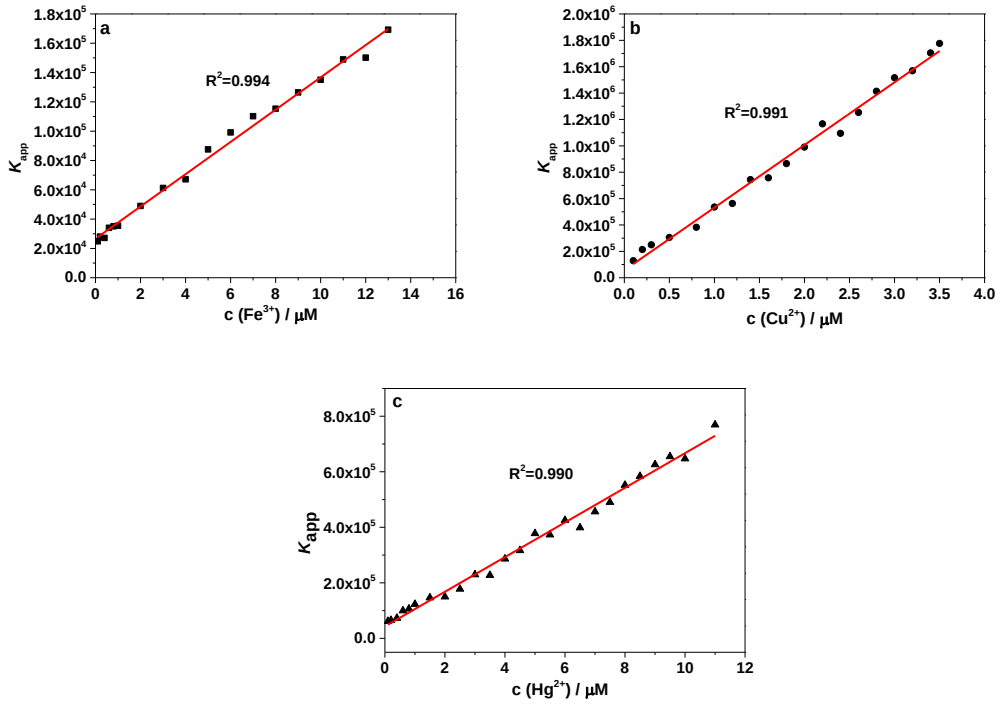

Fig. S6. Plots of the apparent quenching constant (K_{app}) with the functions of (A) Fe^{3+}, (B) Cu^{2+} and (C) Hg^{2+} at different concentrations.

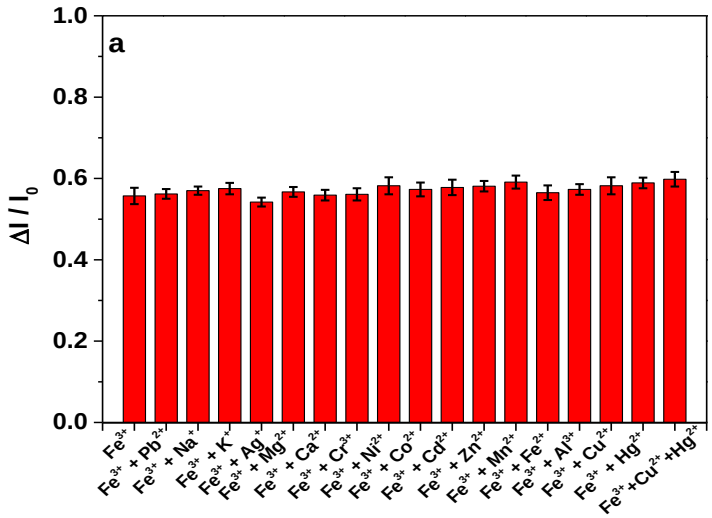

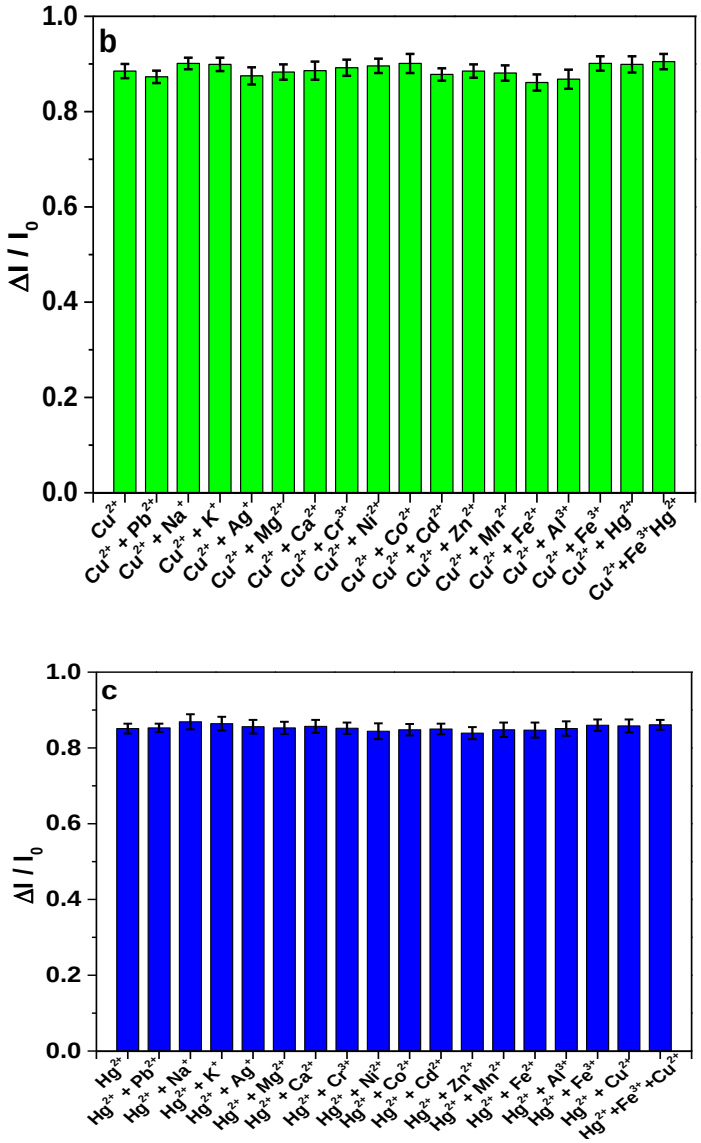

Fig. S7. The competition assays of the polyDOPA-FONs for the detection of a) 13 μM Fe^{3+}, b) 3.5 μM Cu^{2+} and c) 11 μM Hg^{2+} with the coexistence of 30 μM other coexisted metal ion.

Table S1. Formation constants at 25 °C. [3, 4]

Ligand	cations	ML	ML_2	ML_3	T, *I*
		$\log(\beta_1)$	$\log(\beta_2)$	$\log(\beta_3)$	
Acetate	Fe^{3+}	3.38	3.10	1.80	25, 0.0
	Cu^{2+}	2.21	1.42	/	25, 0.0
	Hg^{2+}	3.74	/	/	25, 0.1
Phosphate	Fe^{3+}	9.35	/	/	25, 0.6
	Cu^{2+}	/	/	/	/
	Hg^{2+}	/	/	/	/
Oxalate	Fe^{3+}	7.58	6.23	4.80	25, 1.0
	Cu^{2+}	4.50	8.90	/	25, 0.5
	Hg^{2+}	/	/	/	/
Hydroxide	Fe^{3+}	11.81	11.50	/	25, 0
	Cu^{2+}	6.5	/	/	25, 0
	Hg^{2+}	10.60	11.20	/	25, 0

Table S2. Results from the detections of three metal ions in water samples (n=3)

Entry	Target ions	Added (μM)	Found (μM)	Recoveries (%)	RSD (%)
Tap water	Fe^{3+}	0.0	1.31	/	/
		6.0	7.62	105.17	2.23
		9.0	10.67	104.00	6.48
	Cu^{2+}	0.0	ND[a]	/	/
		1.0	1.01	101.00	2.83
		3.0	3.23	107.67	3.25
	Hg^{2+}	0.0	ND	/	/
		6.0	6.21	103.50	4.12
		9.0	8.47	94.11	4.36
Slender west lake	Fe^{3+}	0.0	3.14	/	/
		6.0	9.01	97.83	3.00
		9.0	12.36	102.39	2.73
	Cu^{2+}	0.0	ND	/	/
		1.0	1.02	102.00	2.12
		3.0	3.02	100.67	3.16
	Hg^{2+}	0.0	ND	/	/
		6.0	6.03	100.50	5.15
		9.0	9.61	106.78	4.58

ND: Not detected.

Reference

1 H. Li, H. Guan, H. Dai, Y. Tong, X. Zhao, W. Qi, S. Majeed, G. Xu, Talanta, 2012, **99**, 811-815.

2 B. X. Shi, Y. Wang, K. Zhang, T. L. Lam, H. L. W Chan, Biosens. Bioelectron. 2011,

26, 2917-2921.

3 S. M. Robert, A. E. Martell, *Critical stability constants,* Springer, 1989.

4 D. A. Skoog, *Fundamentals of analytical chemistry*, Cengage-Brooks/Cole, 2012.